Appl Phys B (2009) 97: 251–255
DOI 10.1007/s00340-009-3697-3

Applied Physics B
Lasers and Optics

Femtosecond laser written stress-induced Nd:$Y_3Al_5O_{12}$ (Nd:YAG) channel waveguide laser

J. Siebenmorgen · K. Petermann · G. Huber · K. Rademaker · S. Nolte · A. Tünnermann

Received: 17 April 2009 / Revised version: 12 June 2009 / Published online: 15 September 2009

Abstract Single tracks and pairs of tracks were written into undoped and Nd-doped YAG crystals using a commercial femtosecond laser system delivering pulses with pulse duration of 140 fs and pulse energies up to 10 μJ. The pulses were focused by a 50× microscope objective below the surface of the crystals. Due to the elasto-optical effect, stress-induced birefringence was observed in domains surrounding the single tracks and between the pairs of tracks. Waveguiding was demonstrated in certain channels in these domains. To investigate the underlying guiding mechanism highly selective chemical etching of the modified material was performed with etching rates up to 5 μm/h. Pumped at 808 nm, laser operation at a wavelength of 1064 nm was achieved. The maximum output power was 25.5 mW at 261 mW of launched pump power with a slope efficiency of 23%.

PACS 42.55.Rz · 42.79.Gn · 42.25.Lc

1 Introduction

Femtosecond lasers are widely used for three-dimensional volume microstructuring of dielectric materials due to nonlinear absorption processes. In recent years, many groups succeeded in inscribing waveguides in different glasses and crystals by producing a permanent change of the refractive index [1–5].

J. Siebenmorgen (✉) · K. Petermann · G. Huber
Institut für Laser-Physik, Universität Hamburg, Luruper Chaussee 149, 22761 Hamburg, Germany
e-mail: jsiebenm@physnet.uni-hamburg.de

K. Rademaker · S. Nolte · A. Tünnermann
Institut für Angewandte Physik, Friedrich-Schiller-Universität Jena, Max-Wien-Platz 1, 07743 Jena, Germany

The fabrication of buried channel waveguides inside these materials is of particular interest for the production of passive and active optical devices. In combination with low-loss waveguiding structures waveguide lasers were demonstrated in glass and different crystalline materials [6–8]. A dielectric crystalline waveguide laser offers many advantages, such as high optical gain, high damage threshold, and in general good overlap between pump mode and laser mode.

Neodymium-doped YAG ($Y_3Al_5O_{12}$) crystals are interesting for inscribing waveguiding structures and realizing waveguide lasers due to the excellent thermomechanical and optical properties, such as high emission cross-section, long fluorescence lifetime, good thermal conductivity, and high mechanical stability. Recently, Nd-doped YAG waveguide lasers in single crystals and ceramics fabricated by direct femtosecond laser writing have been demonstrated by different groups [7, 8]. However, in contrast to those results the underlying waveguiding mechanism is based on a stress induced change of the refractive index in this work.

2 Waveguide fabrication

To produce stress-induced waveguides a chirped pulse amplified femtosecond laser system (Clark-MRX CPA-2010) providing laser pulses at a wavelength of 775 nm, a pulse duration of 140 fs, a pulse energy of 1 mJ, and a repetition-rate of 1 kHz was used. The laser pulses were focused 300 μm below the polished surface of the undoped and neodymium-doped YAG crystals using a 50× microscope objective with a numerical aperture (NA) of 0.70. For the writing process, the crystals were moved transversally with a velocity of 10 μm/s by a motorized translation stage (Fig. 1). Single tracks were inscribed with increasing pulse energies from 1

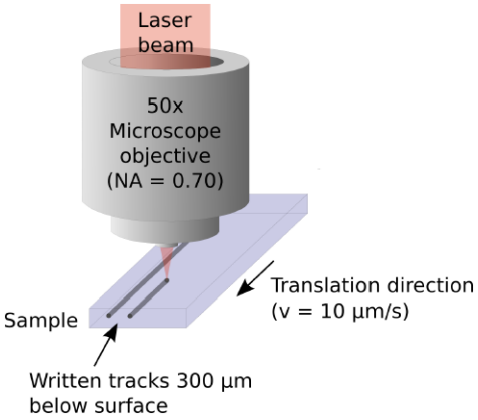

Fig. 1 Schematic of the femtosecond laser writing setup

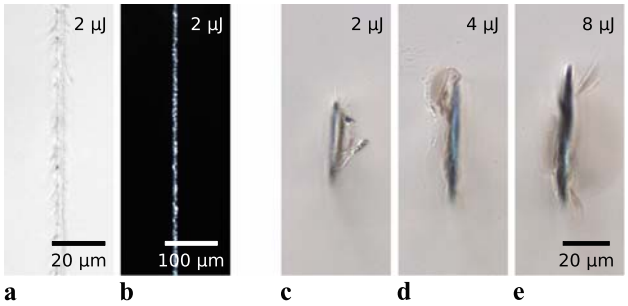

Fig. 2 Microscope images of written single tracks in Nd:YAG: bright field (**a**) and dark field (**b**); cross section perpendicular to the inscribed tracks from 2 to 8 µJ pulse energy in Nd:YAG (**c**)–(**e**)

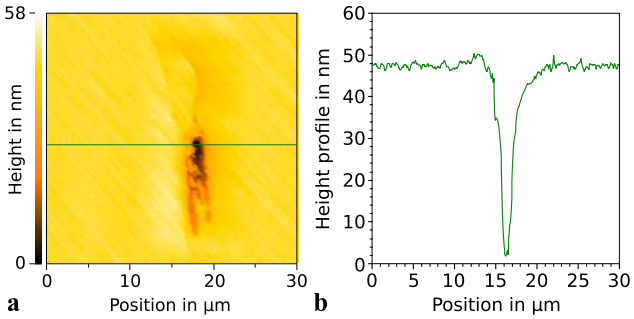

Fig. 3 AFM image of a single line written in undoped YAG at a pulse energy of 1 µJ (**a**); and height profile along the indicated line (**b**)

up to 10 µJ. Additionally, pairs of tracks with a pulse energy of 1.5 µJ and distances between 10 and 30 µm were written. The length of the tracks was about 9 mm after polishing the end facets of the crystal. The diameter of the focal point was calculated to be 6 µm.

3 Results

Structural changes resulting in visible tracks were produced in the crystals. The threshold pulse energy for these modifications was about 1 µJ. Below the damage threshold no material modification was observed.

Figures 2(a) and 2(b) show a microscope image of a track written in undoped YAG at 2 µJ of pulse energy. In Figs. 2(c)–(e) the cross sections of the inscribed tracks are shown. With increasing pulse energy both height and width of the tracks increase and their shape becomes more irregular. The track corresponding to a pulse energy of 2 µJ is 40 µm in height and 5 µm in width. This correlates directly with the focal spot size.

In all samples the formation of cracks during the writing process was observed. With increasing pulse energy these cracks become more distinct up to an extent of 40 µm.

A dark field microscope image of the undoped YAG crystal is shown in Fig. 2(b). All written tracks are visible as bright, grainy traces due to light scattering at the crystal defects. These defects are the result of a destruction of the crystalline structure in the focus of the laser beam. In Fig. 3 an image obtained by an atomic force microscope (AFM) and a height profile of the polished surface of the undoped YAG crystal perpendicular to a track written with a pulse energy of 2 µJ are shown. The image shows the center of the track as a pit with a depth of 46 nm and a FWHM of approximately 1.4 µm.

Formation of these pits can be explained by melting of the material. This is caused by the high temperature in the focus of the laser pulses resulting from creation of a hot electron plasma and the transfer of this energy to the lattice. After cooling down, the melt recrystallizes in a polycrystalline YAG structure rich in lattice defects. These lattice defects cause an expansion of the lattice resulting in lower density and hardness of the material [9]. When polishing the surface, this material could be removed more easily and the pits are left behind.

Another explanation for these structures could be the occurrence of micro explosions at the focal spot, which push material outwards under high pressure. Formation of voids surrounded by densified material is the result of this process [10]. In both cases the inscribed tracks apply high pressure to the surrounding material and thus generate stress. Optically isotropic materials like YAG become anisotropic in this way. Due to the elasto-optical effect, local changes of the refractive index of the surrounding area should occur.

In Fig. 4 microscope images of undoped and Nd-doped YAG crystals under crossed polarizers are shown. Regions without stress remain dark in the images, while the bright white color surrounding the written tracks indicate regions with stress-induced birefringence. With increasing pulse energy the size of the area surrounding each single track increases (Fig. 4(a)). Pairs of tracks show birefringence too (Fig. 4(b)). Due to limitations of the microscope used, no

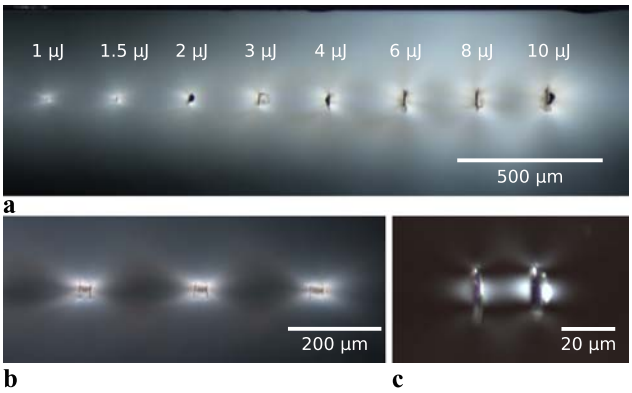

Fig. 4 Microscope image of single tracks in undoped YAG between crossed polarizers (**a**); pairs of tracks in Nd:YAG (**b**) and single pair of tracks in a 45-µm thin undoped YAG sample (**c**)

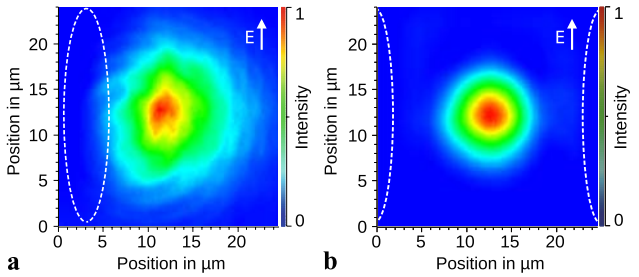

Fig. 5 Near-field images of waveguiding in a 9-mm long channel in Nd:YAG obtained by a CCD camera; single track (marked as a white dashed area) (**a**) and pair of tracks (**b**)

further information about the region between the tracks can be obtained from this 9-mm long crystal. Therefore, a thin sample was cut from a structured crystal and polished mechanically to a thickness of 45 µm. An image of this sample between crossed polarizers is shown in Fig. 4(c). Strong birefringence can be also observed between each double-track structure.

4 Waveguide characterization

Due to the change of the refractive index, waveguiding is possible in channels surrounding the inscribed single tracks and in the center of the pairs of tracks, where the refractive index is higher.

Waveguiding experiments were performed by coupling the light of a He–Ne laser at a wavelength of 632.8 nm into the waveguide with a 20× microscope objective (NA = 0.4). The light was polarized parallel to the long axis of the cross section of the written tracks. The backside of the waveguide was imaged by a 50× microscope objective (NA = 0.70) onto a CCD camera. Waveguiding occurs in multiple channels surrounding the written single tracks (white dashed area in Fig. 5(a)). The diameter of these channels is about 14 µm. The transmitted power was about 30% of the incident pump power for the track written at 1.5 µJ pulse energy. With increasing pulse energy the losses of the waveguides rise. Waveguiding was also observed in the center between two adjacent tracks (Fig. 5(b)) and in the surrounding area of this double structure too. The guided mode in the center of the pair structure has a nearly Gaussian profile. The highest transmitted power of 40% of the incident pump power was obtained for a track distance of 25 µm. Coupling efficiencies and waveguide losses were not measured so far, however, detailed investigations are in progress. For further analyses we estimated the coupling efficiency to be 50% corresponding to waveguide losses of 2.5 and 1.1 dB/cm at a wavelength of 632.8 nm for single tracks and the pair structure, respectively. These values are higher than the waveguide losses for a fs-laser written depressed cladding, buried Nd:YAG waveguide (0.2 dB/cm) as well as a waveguide laser fabricated in a Nd:YAG ceramic (0.6 dB/cm) [7, 8]. Typical losses for fs-laser written waveguides in glasses are around 0.2 dB/cm [11].

Waveguiding is only possible if the incident light is polarized parallel to the long axis of the cross section of the written tracks as indicated in Fig. 5.

The change of the refractive index was estimated by assuming a refractive step index profile of the waveguide, measuring the maximum incident angle Θ_m at which no change of the transmitted power is occurring, and using the formula

$$\Delta n \approx \frac{\sin^2 \Theta_m}{2n}, \tag{1}$$

where n is the refractive index of the unstructured sample. The resulting refractive index change of the waveguides is in the order of $\Delta n \approx 1 \times 10^{-3}$. Due to uncertainties of measuring the maximum incident angle an error of 30% was estimated.

5 Chemical etching

To investigate the underlying stress induced guiding mechanism the YAG samples were immersed in 85% orthophosphoric acid at a temperature of 50°C. After several hours of continuous etching, the samples were cleaned in water and the etching depth of the written tracks relative to the end face of the crystal was measured using a microscope. Subsequently the etching process was continued.

In Fig. 6(a) an image of a partially etched track written with a pulse energy of 1 µJ is shown. The etched part of the track is marked. The same track imaged between crossed polarizers is shown in Fig. 6(b). Only the nonetched part of the track still shows strong birefringence whereas the etched part remains black. It was not possible to observe waveguiding in the area surrounding the etched tracks or between a

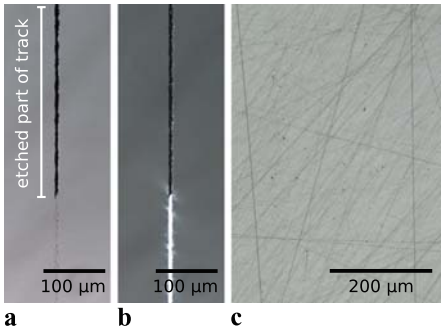

Fig. 6 Microscope images of an etched track written at a pulse energy of 1 µJ (**a**); the same track between crossed polarizers (**b**) damage of the crystal surface after 140 h of etching (**c**)

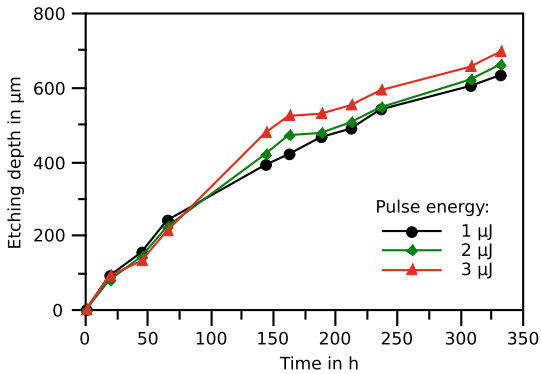

Fig. 7 Evolution of the etching depth of the tracks written with different pulse energies

pair of these tracks due to the absence of a stress-induced change of the refractive index. Further microscope images reveal that only the material of the written tracks were removed. The stress-affected material surrounding the tracks remains unetched. The absence of the birefringence is due to relaxation of the formerly stress-affected material.

After an etching period of 330 h an etching depth between 630 and 700 µm was measured depending on the pulse energy used at the writing process (Fig. 7). With increasing pulse energy and thus increasing cross-section area of the written tracks an increase of the etching rate was observed. All tracks reveal a decreasing etching rate over the time. At the first 19 h etching rates up to 5 µm/h were measured. After 300 h the rate is reduced to about 1 µm/h. The surface of the unmodified material is highly acid resistant. First slight damage of the surface in form of scratches was observed after 140 h (Fig. 6(c)) but even after 300 h of etching the surface remains mostly transparent.

6 Laser experiments

Laser experiments were performed by coupling the light of a Ti:Sapphire laser operating in CW mode at a wavelength

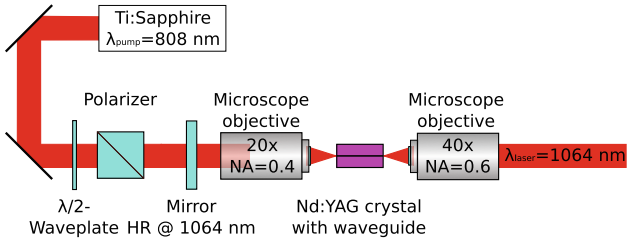

Fig. 8 Schematic of the laser setup

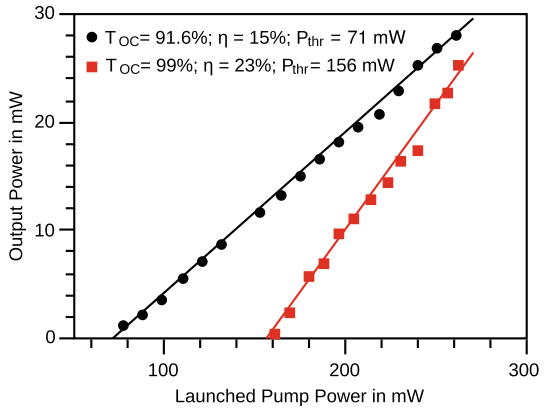

Fig. 9 Laser power as a function of launched pump power for two different output coupling rates

of 808 nm into a waveguide by a 20× microscope objective (NA = 0.4). A $\lambda/2$ waveplate and a polarizer were used to control the polarization and the power of the laser beam (Fig. 8).

In a first experiment laser operation at a wavelength of 1064 nm was achieved without mirrors but using only the Fresnel reflection of about 9% at each surface. Thus, the total output coupling was about 99%. The laser delivered a maximum combined output power of 25.5 mW at 261 mW of launched pump power (Fig. 9). The slope efficiency was 23%. We also placed a plane incoupling mirror, which was highly reflective for the laser wavelength, between the polarizer and the incoupling microscope objective. In this case the laser cavity is formed by this mirror and the back face of the crystal. The microscope objective, which is now part of the resonator, induces 10% of losses at the laser wavelength of 1064 nm in a single pass. With this setup a maximum output power of 28.3 mW and a slightly reduced slope efficiency of 15% were achieved. The decrease of the slope efficiency can be attributed to the additional losses by back-coupling of the cavity mode. The laser light is polarized parallel to the long axis of the cross section of the written tracks as expected from the waveguide experiments.

In Fig. 10 a CCD camera image of the near field of the guided laser mode is shown. The diameter of the laser mode is 14 µm (at $1/e^2$). The laser mode has a nearly Gaussian intensity profile.

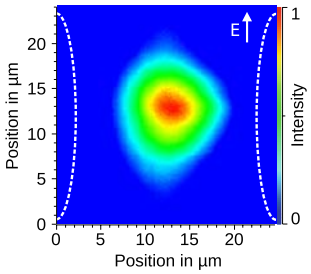

Fig. 10 CCD camera near-field image of the guided laser mode

7 Conclusion

In summary, tracks resulting from a destruction of the crystalline lattice have been written in undoped and Nd-doped YAG crystals using tightly focused femtosecond pulses. Waveguiding was observed due to stress-induced birefringence in the surrounding region of the tracks and between pairs of tracks. The mode guided between a pair of tracks has a nearly Gaussian intensity profile. The refractive index change of these waveguides was estimated to be in the order of 10^{-3}. Etching experiments with etching rates up to 5 µm/h reveal that without stress-induced birefringence waveguiding is no longer possible. Laser operation at a wavelength of 1064 nm was achieved between the end faces of the crystal with a maximum output power of 25.5 mW at 261 mW of launched pump power. The slope efficiency was 23%.

The output power of the waveguide laser was only restricted by the available launched pump power. By using a pump source with higher laser power and optimizing the coupling efficiency, higher waveguide laser output power should be obtained. Experiments with mirrors evaporated directly on the crystal to reduce resonator internal losses are in progress.

Since the formation of fs-laser written waveguides in YAG crystals is independent of the doping ion, this host material is promising to realize waveguide lasers with other rare-earth elements, such as ytterbium or erbium, as active ions.

Acknowledgement This work was supported by the Deutsche Forschungsgemeinschaft (Graduate School 1355 and Leibniz program).

References

1. K.M. Davis, K. Miura, N. Sugimoto, K. Hirao, Opt. Lett. **21**, 1729 (1996)
2. C.N. Borca, V. Apostolopoulos, F. Gardillou, H.G. Limberger, M. Pollnau, R.-P. Salathé, Appl. Surf. Sci. **253**, 8300 (2007)
3. J. Burghoff, C. Grebing, S. Nolte, A. Tünnermann, Appl. Phys. Lett. **89**, 081108 (2006)
4. A.H. Nejadmalayeri, P.R. Herman, J. Burghoff, M. Will, S. Nolte, A. Tünnermann, Opt. Lett. **30**, 964 (2005)
5. K. Itho, W. Watanabe, S. Nolte, C.B. Schaffer, MRS Bull. **31**, 620 (2006)
6. S. Taccheo, G. Della Valle, R. Osellame, G. Cerullo, N. Chiodo, P. Laporta, O. Svelto, Opt. Lett. **29**, 2626 (2004)
7. A.G. Okhrimchuk, A.V. Shestakov, I. Khrushchev, J. Mitchell, Opt. Lett. **30**, 2248 (2005)
8. G.A. Torchia, A. Rodenas, A. Benayas, E. Canelar, L. Roso, D. Jaque, Appl. Phys. Lett. **92**, 111103 (2008)
9. R. Balzer, H. Peisl, W. Waidelich, Z. Phys. **204**, 405 (1967)
10. E.N. Glezer, E. Mazur, Appl. Phys. Lett. **71**, 882 (1997)
11. M. Ams, G.D. Marshall, P. Dekker, M. Dubov, V.K. Mezentsev, I. Bennion, M.J. Withford, IEEE Sel. Top. Quantum Electron. **14**, 1370 (2008)